

# Incorporating Nonlinear Lumped Elements into the Unconditionally Stable FETD Method

Bruno R. de Souza, Wilson A. Artuzi Jr. and Marlio J. C. Bonfim

Departamento de Engenharia Elétrica - Universidade Federal do Paraná

*Abstract*— An approach to incorporate the nonlinear equivalent circuit model of a Schottky diode in finite element time domain simulations is proposed. The approach consists in decoupling the linear system of equations resulting from the finite element method and the nonlinear equations of the diode model. It is shown by numerical experiments that the approach is valid for practical diode parameters.

*Keywords*— FETD, bilinear transformation, vector wave equation, conjugate gradient, Schottky diode

## I. INTRODUCTION

In the context of microwave circuit integration, numerical analyses need to be performed in order to verify the full-wave behavior of a designed system prior to its fabrication. There exists a variety of frequency domain numerical methods that can be used for this purpose [1]. Though these methods are able to deal with dispersive materials and lumped networks, they have limited performance when the nonlinear behavior becomes predominant. On the other hand, the finite difference and the finite element time domain (FDTD and FETD) methods [2] can naturally incorporate the nonlinear behavior, but the dispersive characteristic implementation is not straightforward. Techniques like the piecewise linear recursive convolution, auxiliary differential equation and bilinear transformation have been successfully implemented in both FDTD and FETD codes to deal with the dispersion problem [3]. Their common disadvantage is the condition for stability which constraints the time step to a maximum allowable value. The Newmark Beta integration technique has eliminated the time step constraint in FETD making it an attractive tool to analyze integrated circuits of increased complexity in size and geometry [4], [5]. The objective of this paper is to present a technique that incorporates both dispersive and nonlinear characteristics of a lumped diode into the unconditionally stable FETD method. Validation of the proposed methodology is conducted by an example consisting of a Schottky diode rectifier. Numerical comparison with circuit simulator results reveal the technique is accurate for practical applications while preserving numerical stability.

## II. FORMULATION

### A. Finite Element Method

In the present formulation,  $s = j2\pi f$  is the complex frequency and  $z$  is the z-transform variable. The finite element procedure applied to the electric field vector wave

This work was partially supported by CNPq with a PIBIC research grant to Bruno R. Souza. Contacts: souza.brs@gmail.com, artuzi@eletrica.ufpr.br, marliob@eletrica.ufpr.br

equation using edge linear basis functions results in an equivalent electric circuit matrix equation of the form

$$\left( sC + G + \frac{1}{s}K \right) v + p i_d = i_s \quad (1)$$

where the entries of vectors  $i_s$  and  $v$  are the known excitation current sources and the unknown voltages on the edges of the finite element mesh, respectively [6]. The entries of matrices  $C$ ,  $G$  and  $K$  relate pairs of basis functions  $\vec{W}_k$  and  $\vec{W}_l$  as

$$C_{kl} = \int_V \varepsilon \vec{W}_k \cdot \vec{W}_l dV \quad (2)$$

$$G_{kl} = \oint_S \sigma_s \hat{n} \times \vec{W}_k \cdot \hat{n} \times \vec{W}_l dS \quad (3)$$

$$K_{kl} = \int_V \frac{1}{\mu} \nabla \times \vec{W}_k \cdot \nabla \times \vec{W}_l dV \quad (4)$$

where  $\varepsilon$  and  $\mu$  are the electric permittivity and magnetic permeability in the computational domain  $V$  and  $\sigma_s$  is the surface conductivity of the domain boundary  $S$  being  $\hat{n}$  the normal unit vector outward  $S$ . The diode is assumed to be connected in parallel with one edge of the mesh, thus the entries of vector  $p$  are all zeros except for the value one in the row corresponding to the edge where the diode is placed. The diode equivalent circuit model is shown in

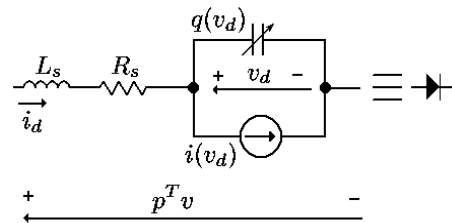


Fig. 1. Equivalent circuit model of the diode.

Fig. 1 and it is described mathematically by the nonlinear system

$$p^T v = sL_s i_d + R_s i_d + v_d \quad (5)$$

$$i_d = i(v_d) + sq(v_d) \quad (6)$$

with

$$i(v_d) = I_s (e^{v_d/NV_T} - 1) \quad (7)$$

$$q(v_d) = C_{jo} \left[ v_d + |v_d| - \frac{V_j}{1-M} \left( 1 + \frac{|v_d|}{V_j} \right)^{1-M} \right] \quad (8)$$

where the Schottky diode parameters  $L_s$ ,  $R_s$ ,  $I_s$ ,  $N$ ,  $V_T$ ,  $C_{jo}$ ,  $V_j$  and  $M$  have their corresponding meanings in common circuit simulators [7]. Equations (7) and (8) have continuous derivatives with respect to  $v_d$  and the last represents the depletion charge only since the diffusion charge can be neglected in Schottky diodes.

### B. Decoupling

In order to solve (1) in the discrete time domain, it will be convenient to make

$$v = s w \quad (9)$$

and add the term

$$\frac{1}{L_s} p p^T w \quad (10)$$

to both sides of (1) to form, together with (5) and (6), the system of equations

$$\left( s^2 C + sG + K + \frac{1}{L_s} p p^T \right) w = i_e - p i_d + \frac{1}{L_s} p p^T w \quad (11)$$

$$v_d + R_s i_d + s L_s i_d - s p^T w = 0 \quad (12)$$

$$i_d - i(v_d) - s q(v_d) = 0 \quad (13)$$

Coupling among the large linear system of equations (11) and the small nonlinear system formed by (12) and (13) becomes looser as the value of  $L_s$  increases. Based on this property, it can be possible to solve the small nonlinear system apart depending upon the value of  $L_s$ .

### C. Time Domain Solution

The discrete time domain solution of the system formed by (11) to (13) arises after its mapping to the z-domain using the bilinear transformation

$$s = \frac{2}{\Delta t} \frac{1 - z^{-1}}{1 + z^{-1}} \quad (14)$$

followed by the inverse z-transform given by the property

$$z^{-k} f \leftrightarrow f^{n-k+1} \quad (15)$$

where  $\Delta t$  is the time step and the index  $n - k + 1$  represent the time instant  $(n - k + 1)\Delta t$  [8].

The procedure outlined above is equivalent to convert the system of equations to the continuous time domain and then apply the Newmark Beta integration with  $\beta = 1/4$  in (11) and the trapezoidal integration in (12) and (13), which are known to be unconditionally stable methods regardless of the time step size [4].

After some algebraic manipulation, it is obtained the linear set of difference equations

$$\left[ C + \frac{\Delta t}{2} G + \frac{\Delta t^2}{4} \left( K + \frac{1}{L_s} p p^T \right) \right] w^n = i_e^n - p i_d^n - G v^{n-1/2} - K w^n \quad (16)$$

$$v^{n+1/2} = v^{n-1/2} + \Delta t u^n \quad (17)$$

$$w^{n+1} = w^n + \Delta t v^{n+1/2} \quad (18)$$

$$V = v_d^{n+1} + v_d^n + R_s (i_d^{n+1} + i_d^n) + \frac{2}{\Delta t} L_s (i_d^{n+1} - i_d^n) - 2v^{n+1/2} \quad (19)$$

$$I = i_d^{n+1} + i_d^n - i(v_d^{n+1}) - i(v_d^n) - \frac{2}{\Delta t} [q(v_d^{n+1}) - q(v_d^n)] \quad (20)$$

The approximation

$$\frac{1}{4} (f^{n+1} + 2f^n + f^{n-1}) \approx f^n \quad (21)$$

in the right-hand side of (16) is responsible for the decoupling of equation (16) and the nonlinear system formed by (19) and (20), however, it can corrupt the solution if small values of  $L_s$  are involved. Fortunately, acceptable values are encountered in practice as it will be illustrated with the example of next section. The conjugate gradient method with diagonal preconditioning is used to solve (16) in each time step [5]. The wanted responses for the excitation currents are the voltages on the edges of the mesh being updated in (17). Before calculating the next time step, it is necessary to solve the nonlinear system where  $V$  and  $I$  are residuals that must be minimized to obtain the updates of  $v_d$  and  $i_d$ . The Newton's method provided by

$$\begin{bmatrix} v_d^{n+1} \\ i_d^{n+1} \end{bmatrix}_{m+1} = \begin{bmatrix} v_d^{n+1} \\ i_d^{n+1} \end{bmatrix}_m - \begin{bmatrix} \frac{\partial V}{\partial v_d^{n+1}} & \frac{\partial V}{\partial i_d^{n+1}} \\ \frac{\partial I}{\partial v_d^{n+1}} & \frac{\partial I}{\partial i_d^{n+1}} \end{bmatrix}_m^{-1} \begin{bmatrix} V \\ I \end{bmatrix}_m \quad (22)$$

with the initial guesses

$$\begin{bmatrix} v_d^{n+1} \\ i_d^{n+1} \end{bmatrix}_1 = \begin{bmatrix} v_d^n \\ i_d^n \end{bmatrix} \quad (23)$$

has been used to perform the task.

## III. EXPERIMENT

A Schottky diode rectifier is constructed in order to verify the performance of the proposed technique. The structure is formed by two sections of 50  $\Omega$  microstrip transmission lines cascaded in series with a Schottky diode. The diode is mounted on a socket and BNC connectors are provided at the transmission line ends to apply the sinusoidal source output and the digital oscilloscope input having both 50  $\Omega$  impedances. The circuit schematic is outlined in Fig. 2.

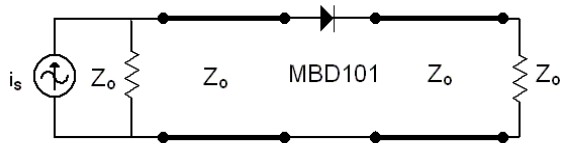


Fig. 2. Equivalent circuit of the diode connected in series with a microstrip transmission line.

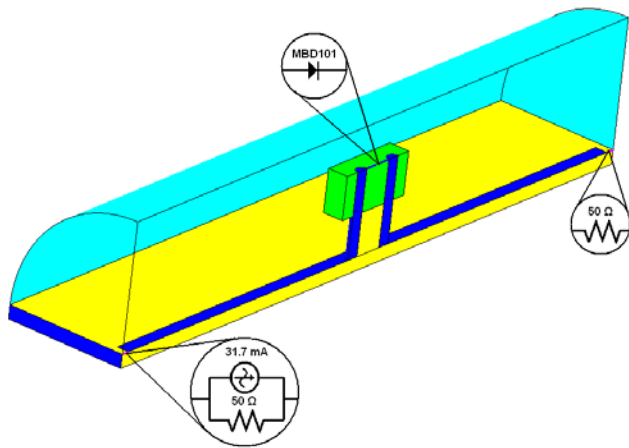


Fig. 3. Finite element model of the diode connected in series with a microstrip line, including the socket. Only half structure is modelled due to symmetry.

### A. Modeling

Half section of the structure geometrical model is shown in Fig. 3. The 40 mm long microstrip line has a width 2.5 mm etched on a FR4 substrate having 0.8 mm of thickness and a dielectric constant of 4.5. There is a gap of 1 mm in the middle of the transmission line where a 5 mm high socket made of two cylindrical metallic pins is soldered. The cylinders have 0.75 mm of diameter and have their axes spaced of 2.55 mm. The highest half of the socket has a polyethylene insulator with a dielectric constant of 4. The computational space is delimited by a cylindrical surface having a radius of 8 mm. The metallic surfaces are modeled with  $\sigma_s = 10^6\ \text{S/m}$ . Non metallic boundaries are modelled as perfect magnetic walls ( $\sigma_s = 0$ ). The source and load impedances of  $50\ \Omega$  are obtained by adding conductance values of 0.01 S to the elements  $G_{kl}$  in (3) where  $k = l$  are the indices of their corresponding edges of the finite element mesh that lay on 0.5 mm gaps at the transmission line ends. A sinusoidal current source having a peak of 31.7 mA and a frequency of 500 MHz is applied to one of these gaps. The MBD101 Schottky diode is placed in the line that connects the two cylinders on the top of the socket. The diode parameters are  $L_s = 0.1\ \text{nH}$ ,  $R_s = 0.1\ \Omega$ ,  $I_s = 19\ \text{nA}$ ,  $V_T = 25\ \text{mV}$ ,  $C_{j0} = 0.89\ \text{pF}$ ,  $V_j = 0.75\ \text{V}$  and  $M = 0.1$ .

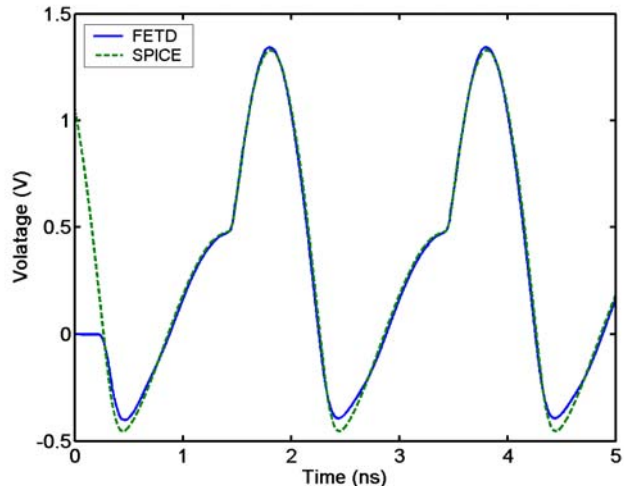


Fig. 4. Comparison of calculated voltages on the load against time (— FETD, - - SPICE).

### B. Numerical Results

First, the rectifier structure is simulated with a tetrahedral mesh having an average edge length of 5 mm and a time step of 3.0 ps. The mesh is refined over regions of geometric details. The voltage response across the  $50\ \Omega$  load is sampled and it is plotted with solid line in the graph of Fig. 4. For comparison, the voltage response has been calculated with a SPICE circuit simulator using the same diode parameters. In order to include the effect of parasitic reactances of the socket in the circuit simulator, a series inductance  $L_p = 3.8\ \text{nH}$  is been added to the series inductance of the diode  $L_s$  and a capacitance  $C_p = 0.18\ \text{pF}$  is placed in parallel with the diode. These values are calculated analytically based on the parallel wire transmission line formulas [7]. The obtained curve is plotted with dashed line in the same graph of Fig. 4. As it can be seen, good agreement is achieved and the differences can be attributed to other parasitic reactances that were not taken into account in the SPICE circuit simulation.

To verify the effects of time step size  $\Delta t$  and diode series inductance  $L_s$  in the finite element simulations, the power spectrum on the  $50\ \Omega$  load is calculated for better comparison. In the bar graph of Fig. 5, it is shown the results simulated with different time steps together with the SPICE result. As it is expected, better agreement is observed as the time step is reduced. In the bar graph of Fig. 6, two additional simulations have been performed with  $L_s = 0.01\ \text{nH}$  and  $L_s = 0.001\ \text{nH}$ . Though the response is stable, the error increases as the value of  $L_s$  is decreased, as mentioned in section II. Nevertheless, practical values of  $L_s$  are usually in the range of 0.1 nH, thus the proposed method can be applied.

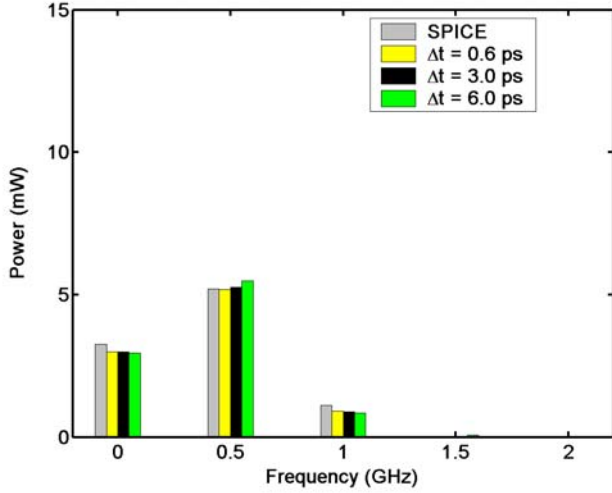


Fig. 5. Power spectrum on the load for different time step sizes and  $L_s = 0.1$  nH.

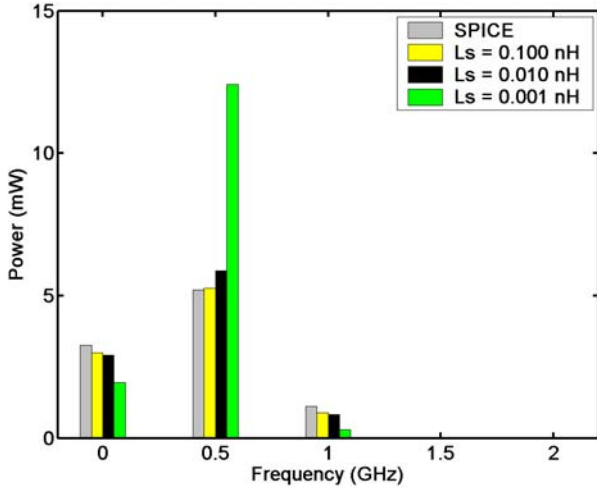


Fig. 6. Power spectrum on the load for different values of  $L_s$  and  $\Delta t = 3.0$  ps.

#### IV. CONCLUSIONS

An approach for incorporating nonlinear lumped elements in FETD simulations has been presented using a Schottky diode as an example. The FETD system of linear equations is decoupled from the diode nonlinear circuit equations to enhance the computational speed. Numerical experiments in comparison with circuit simulator results have shown that the approach is valid for diode lead inductances larger than 0.01 nH, which is an acceptable value in most practical situations. Experiments should be carried out to complete the validation of the proposed method.

#### REFERENCES

- [1] R. Sorrentino, *Numerical Methods for Passive Microwave and Millimeter Wave Structures*, IEEE Press, New York, 1989.
- [2] A. Taflov, *Computational Electrodynamics: The Finite-Difference Time-Domain Method*, Artech House, Boston, 1995.
- [3] S. Liu, N. Yuan and J. Mo, "A novel FDTD formulation for dispersive media", *IEEE Microwave and Wireless Comp. Lett.*, vol.13, pp.187-189, May 2003.
- [4] S. D. Gedney and U. Navsariwala, "An unconditionally stable finite element time-domain solution of the vector wave equation," *IEEE Microwave and Guided Wave Lett.*, vol.5, pp.332-334, Oct. 1995.
- [5] W. A. Artuzi Jr., "Improving the Newmark time integration scheme in finite element time domain methods," *IEEE Microwave and Wireless Comp. Lett.*, vol.15, pp.898-900, Dec. 2005.
- [6] J. P. Webb, "Edge elements and what they can do for you," *IEEE Trans. Magn.*, vol.29, pp.1460-1465, Mar. 1993.
- [7] I. Bahl and P. Bhartia, *Microwave Solid State Circuit Design*, John Wiley & Sons, 1988.
- [8] A. V. Oppenheim, R. W. Schaffer and J. R. Buck, *Discrete-Time Signal Processing*, Prentice-Hall, 1999.